NUMB as a Therapeutic Target for Melanoma

Hristova, Denitsa M. ; Fukumoto, Takeshi ; Takemori, Chihiro ; Gao, Le ; Hua, Xia ; Wang, Joshua X. ; Li, Ling ; Beqiri, Marilda ; Watters,…

(Citation)
Journal of Investigative Dermatology,142(7):1882-1892.e5

(Issue Date)
2022-07

(Resource Type)
journal article

(Version)
Version of Record

(URL)
https://hdl.handle.net/20.500.14094/90009396

NUMB as a Therapeutic Target for Melanoma

Denitsa M. Hristova[1], Takeshi Fukumoto[1,2,4], Chihiro Takemori[2], Le Gao[3], Xia Hua[1], Joshua X. Wang[1], Ling Li[1], Marilda Beqiri[1], Andrea Watters[1], Adina Vultur[1], Yusra Gimie[1], Vito Rebecca[1], Anastasia Samarkina[1], Haruki Jimbo[2], Chikako Nishigori[2], Jie Zhang[3], Chaoran Cheng[3], Zhi Wei[3], Rajasekharan Somasundaram[1], Mizuho Fukunaga-Kalabis[1,4] and Meenhard Herlyn[1,4]

JID Open

The upregulation of the adaptor protein NUMB triggers melanocytic differentiation from multipotent skin stem cells, which share many properties with aggressive melanoma cells. Although NUMB acts as a tumor suppressor in various human cancer types, little is known about its role in melanoma. In this study, we investigated the role of NUMB in melanoma progression and its regulatory mechanism. Analysis of The Cancer Genome Atlas melanoma datasets revealed that high *NUMB* expression in melanoma tissues correlates with improved patient survival. Moreover, NUMB expression is downregulated in metastatic melanoma cells. *NUMB* knockdown significantly increased the invasion potential of melanoma cells in a three-dimensional collagen matrix in vitro and in the lungs of a mouse model in vivo; it also significantly upregulated the expression of the *NOTCH* target gene *CCNE*. Previous studies suggested that Wnt signaling increases NUMB expression. By mimicking Wnt stimulation through glycogen synthase kinase-3 inhibition, we increased NUMB expression in melanoma cells. Furthermore, a glycogen synthase kinase-3 inhibitor reduced the invasion of melanoma cells in a NUMB-dependent manner. Together, our results suggest that NUMB suppresses invasion and metastasis in melanoma, potentially through its regulation of the *NOTCH–CCNE* axis and that the inhibitors that upregulate NUMB can exert therapeutic effects in melanoma.

Journal of Investigative Dermatology (2022) **142,** 1882–1892; doi:10.1016/j.jid.2021.11.027

INTRODUCTION

Melanoma is a cancer that develops in melanocytes, and the phenotype of advanced-stage melanoma often resembles neural crest precursors, which are the cellular origin of melanocytes in the skin (Li et al., 2010). Most early-stage melanomas localize at the epidermal–dermal interface where normal melanocytes are located. In contrast, advanced metastatic melanoma cells can migrate throughout tissues in a manner similar to that of neural crest cells during vertebrate embryonic development. Furthermore, the molecular signaling pathways critical for normal embryonic development and stem cell maintenance are often reactivated in melanoma cells (Liu et al., 2014). One of them is the NOTCH pathway, which has been implicated in melanoma pathogenesis and in the regulation of adult stem cells. We previously showed that NOTCH plays a role in the self-renewal of multipotent, neural crest–like skin precursors, which is a potential reservoir for skin melanocytes (Fukunaga-Kalabis et al., 2015). Melanocyte differentiation from multipotent precursor cells is stimulated when the precursors are activated by canonical Wnt ligands in combination with mitogens such as stem cell factor and endothelin. The initial step of this differentiation is triggered by upregulated NUMB, which inhibits NOTCH signaling in skin precursors (Fukunaga-Kalabis et al., 2015).

NUMB was identified as a cell-fate determinant in Drosophila embryos, which was later confirmed in vertebrates (Uemura et al., 1989; Zhong et al., 1996). In neurogenesis, NUMB binds to the active form of intracellular NOTCH and inhibits NOTCH-dependent gene expression to repress neuronal differentiation (Wakamatsu et al., 1999). In addition to its role in NOTCH inhibition, NUMB induces p53 expression and it inhibits the Hedgehog signaling pathway, also important players in aggressive melanoma (Colaluca et al., 2008; Di Marcotullio et al., 2006). NUMB has been suggested to suppress tumors in several cancers, where NUMB expression is frequently downregulated in malignant cells (Pece et al., 2011). In melanoma, NUMB is a target of microRNA-146a, which has an oncogenic role (Forloni et al., 2014). Moreover, NUMB is required for the stabilization and localization of the cell cycle regulator PLK1, suggesting that dysregulation of NUMB expression can contribute to melanoma development through mitotic errors (Schmit et al., 2012). Because metastatic melanoma cells share embryonic and migratory phenotypes with neural crest–like precursors in the skin, we hypothesized that dysregulation of NUMB is involved not only in melanoma development but also in its progression. In this study, we investigated the biological, mechanistic, and therapeutic role of NUMB in melanoma.

[1]*The Wistar Institute, Philadelphia, Pennsylvania, USA;* [2]*Division of Dermatology, Department of Internal Related, Kobe University Graduate School of Medicine, Kobe, Japan; and* [3]*Department of Computer Science, New Jersey Institute of Technology, Newark, New Jersey, USA*

[4]*These authors contributed equally to this work.*

Correspondence: Takeshi Fukumoto, Division of Dermatology, Department of Internal Related, Kobe University Graduate School of Medicine, 7-5-1 Kusunoki-cho, Chuo-ku, Kobe 650-0017, Japan. E-mail: fuku@med.kobe-u.ac.jp

Abbreviations: GSK-3, glycogen synthase kinase-3; KD, knockdown; lncRNA, long noncoding RNA; shNUMB, short hairpin RNA targeting NUMB

Received 1 April 2021; revised 26 October 2021; accepted 16 November 2021; accepted manuscript published online 7 December 2021; corrected proof published online 22 January 2022

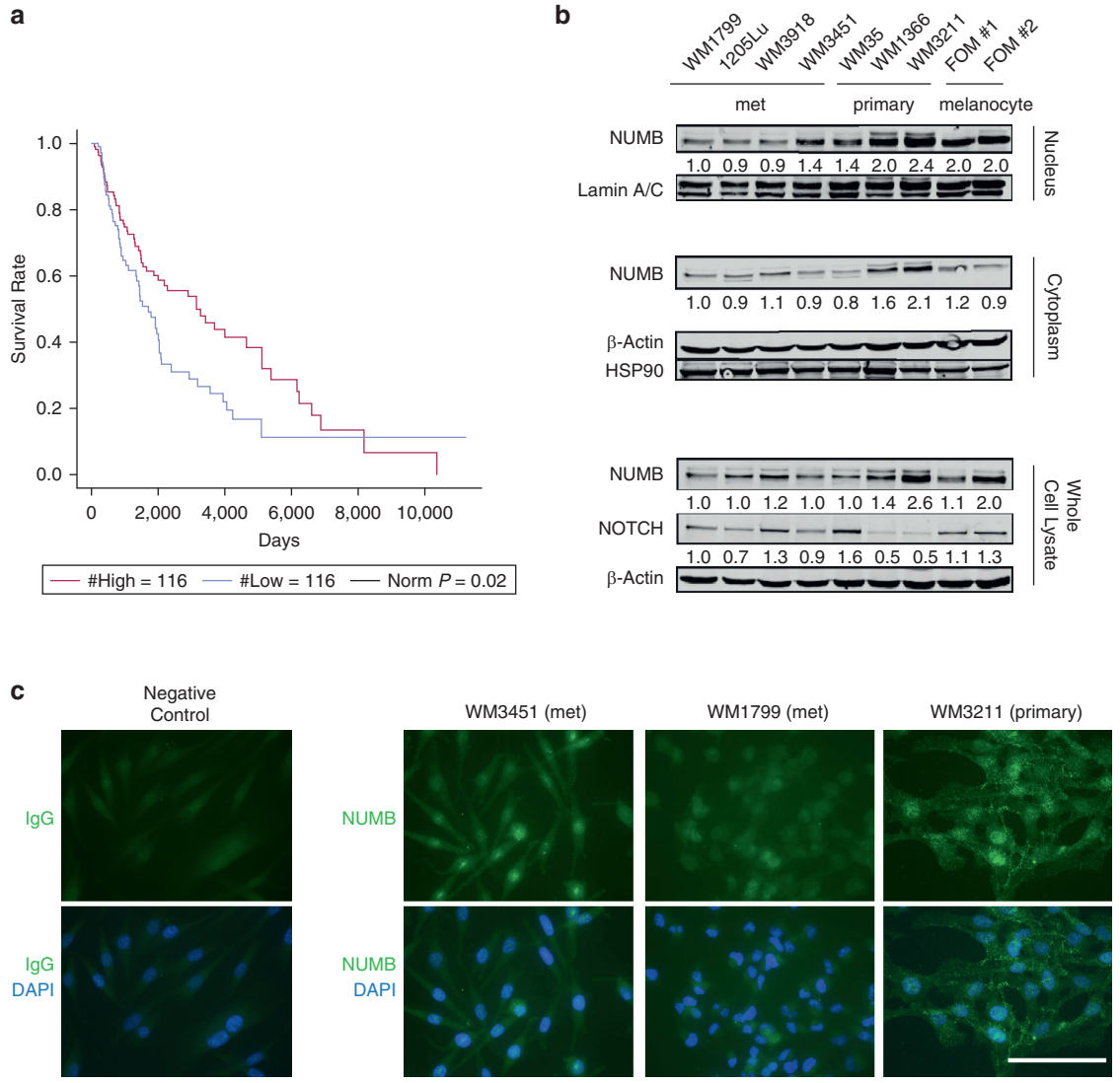

Figure 1. Low *NUMB* levels are correlated with decreased overall survival in patients with melanoma. (**a**) Kaplan–Meier survival curve analysis of the overall survival of patients with low and high *NUMB* mRNA expression in melanoma was used to compare a quarter each of the patients having the highest with those having the lowest *NUMB* expression in their tumor (Cancer Genome Atlas Network, 2015). (**b**) Immunoblot analysis showing NUMB and NOTCH expression in melanocytes (FOM#1 and #2), primary melanoma cell lines (WM35, WM1366, WM3211), and met melanoma cell lines (WM1799, 1205Lu, WM3918, WM3451) in whole-cell lysates, cytoplasmic fractions, or nuclear fractions. Blotting for β-actin, HSP90, and lamin A/C serves as loading controls. The relative intensities of the immunoblot bands were quantified. (**c**) Immunofluorescent staining showing NUMB expression in melanoma cell lines. Bar = 100 μm. met, metastatic.

RESULTS

NUMB expression correlates with melanoma survival and is downregulated in metastatic melanoma cells

First, to investigate the potential involvement of NUMB in melanoma progression, we analyzed melanoma RNA-sequencing data from The Cancer Genome Atlas, together with the patients' clinical information (Cancer Genome Atlas Network, 2015). Kaplan–Meier analyses showed that patients with lower *NUMB* gene expression had significantly decreased overall survival (log-rank test, $P = 0.02$) (Figure 1a). Recent evidence showed the pivotal role of long noncoding RNAs (lncRNAs) in uveal melanoma by regulating proliferation, invasion, and metastasis (Cheng et al., 2016; Milán-Rois et al., 2021). Thus, a second analysis was focused on NUMB lncRNA, which was marginally associated with patient survival ($P = 0.04$, for both log-rank test and the Cox regression) in the 232 The Cancer Genome Atlas samples. To see whether the association of NUMB lncRNA with patient survival is an independent and driving signal or whether it is driven by the correlation between NUMB and NUMB lncRNA, we performed Cox regression with both NUMB and NUMB lncRNA as covariates. Interestingly, we observed that NUMB remained significant ($P = 0.04$), whereas NUMB lncRNA was no longer significant ($P = 0.25$), suggesting that it is NUMB that drives the survival association.

NUMB protein expression was downregulated in three of four metastatic melanoma cell lines in the nucleus. In contrast, two of the three examined primary melanoma cell lines demonstrated similar levels of NUMB expression to

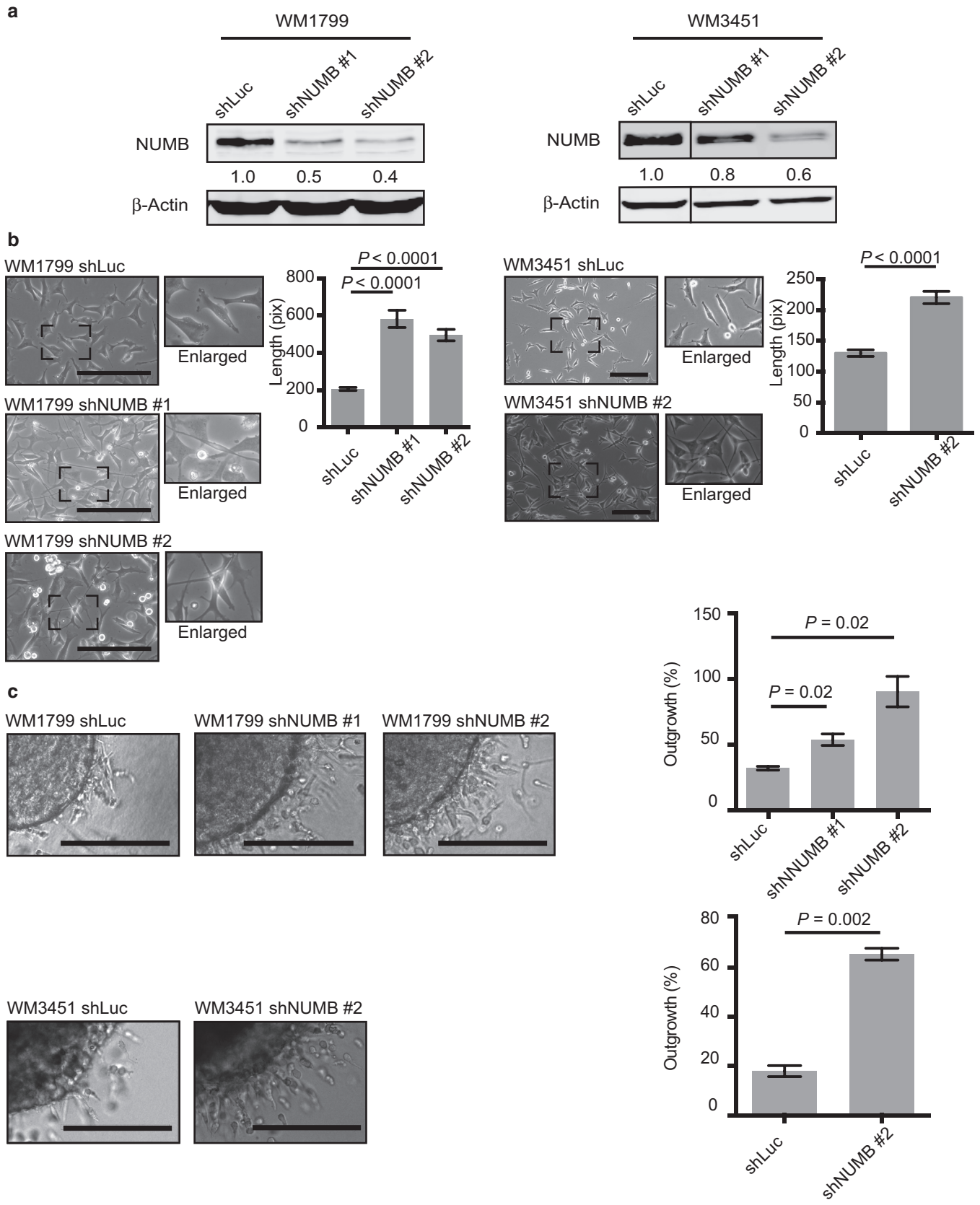

Figure 2. Knockdown of *NUMB* promotes cell invasion in metastatic melanoma cell lines. (**a**) Immunoblot analysis showing NUMB expression in metastatic melanoma cell lines with a control vector (shLuc) or shNUMB #1 and #2. Blotting for β-actin serves as a loading control. The relative intensities of the immunoblot bands were quantified. (**b**) Downregulation of *NUMB* by shRNA in metastatic melanoma cell lines leads to morphological changes, which were quantified. Bar = 200 μm. (**c**) shNUMB-transduced cells or control vector–transduced cells were grown as spheroids embedded in a 3D collagen matrix to test their invasive ability. *NUMB* knockdown cell lines showed increased invasion in WM1799 (on day 1) and WM3451 (on day 2) melanoma cell lines compared

those of normal melanocytes (Figure 1b). These results are consistent with those of a previous study showing that the expression of NUMB is reduced in cancer tissues compared with that in normal tissues, with the reduction even worse in tumor tissues with TNM stages III–IV than in those with stages I–II (Liang et al., 2019). Immunofluorescent staining showed that in the human melanoma cell lines WM1799, WM3451, and WM3211, NUMB was expressed mainly in the nucleus but also in the cytoplasm and cell membrane (Figure 1c). These data suggest that NUMB may function both inside and outside the nucleus.

Previous studies suggested that the activation of NOTCH signaling is necessary for melanoma progression (Aydin et al., 2014; Balint et al., 2005; Liu et al., 2006). Consistent with previous reports, we observed that NOTCH was barely expressed in WM1366 and WM3211 melanoma cells that have a high NUMB expression (Figure 1b) (Choi et al., 2021; Li et al., 2019; Wakamatsu et al., 1999).

Depletion of NUMB increases melanoma invasion and metastasis

To assess whether NUMB downregulation is directly involved in melanoma aggressive behavior, we performed *NUMB* knockdown (KD) experiments. The metastatic melanoma cell lines WM1799 and WM3451 were transfected with lentiviral vectors encoding short hairpin RNAs targeting *NUMB* (shNUMBs) to downregulate NUMB expression (Figure 2a and Supplementary Figure S1a). *NUMB* KD caused morphological changes in the melanoma cells: they became spindle shaped with significantly elongated dendrites resembling mesenchymal cells (Figure 2b and Supplementary Figure S2). *NUMB* KD did not affect the proliferation of WM1799 and WM3451 cells over a 6-day period (Supplementary Figure S1b). To explore whether NUMB affects melanoma invasion, we employed a three-dimensional spheroid model, which represents the complexity and heterogeneity of tumors within tissues (Smalley et al., 2006). *NUMB* KD induced a significant increase in the invasion of melanoma spheroids into collagen matrices (Figure 2c and Supplementary Figure S3a and b). Similar experiments were also performed with the primary melanoma cell line WM35 (Supplementary Figures S2 and S3). *NUMB* KD induced a significant increase in the invasion of melanoma spheroids into collagen matrices, although *NUMB* KD did not affect the proliferation over a 7-day period (Supplementary Figures S2c and S3c).

Next, we sought to investigate whether *NUMB* KD promotes the progression of melanoma in vivo. We tested lung colony formation in an experimental metastasis model by injecting WM1799 melanoma cells intravenously into NOD/SCID IL2Rγ^{null} or NSG mice. After 9 weeks, the mice were euthanized, and lung samples were collected for the detection of metastases. Both the area and the number of metastatic colonies developed in the lungs were found to be increased in mice injected with WM1799 shNUMB cells compared with those found in the WM1799 short hairpin RNA targeting firefly luciferase control cell–injected group (Figure 3). These data suggest that NUMB plays an important role in the invasion and metastatic potential of melanoma.

NUMB is induced by the inhibition of glycogen synthase kinase-3 in melanoma cells

Our KD experiments suggested that NUMB negatively regulates melanoma aggressive behavior. We previously showed that NUMB expression is increased by canonical Wnt ligands (Fukunaga-Kalabis et al., 2015). In this study, we sought to test whether NUMB expression could be increased in melanoma cells by pharmacologically activating the canonical Wnt pathway. To do so, we blocked glycogen synthase kinase-3 (GSK-3), which is a negative regulator of canonical Wnt signaling, using the GSK-3 inhibitor IX. This inhibitor upregulated the expression of NUMB protein in melanoma cell lines and activated β-catenin (Figure 4a). Activation of β-catenin was also confirmed by the upregulation of the mRNA expression of its target gene, *AXIN2* (Supplementary Figure S4). Furthermore, upregulated NUMB was not only found in the cytoplasm but was also colocalized with active β-catenin in the nuclei of WM1799 and WM3451 cells (Figure 4b). These results were consistent with those of previous studies reporting NUMB interaction with β-catenin (Colaluca et al., 2018; Liang et al., 2019).

GSK-3 inhibition decreases melanoma invasion in a NUMB-dependent manner

Previous studies have shown that GSK-3 promotes cell survival, growth, motility, and drug resistance in melanoma cells (Atkinson et al., 2015; John et al., 2012; Kubic et al., 2012; Panka et al., 2008; Smalley et al., 2007; Zimmerman et al., 2013). We sought to investigate the preventive efficacy of GSK-3 inhibitors in melanoma. In the untreated spheroids, the difference in invasion between control and *NUMB* KD was less obvious after >1 week owing to the high rate of invasion and model saturation (Figure 5). However, treatment with 3 μM GSK-3 inhibitor IX was sufficient to inhibit the invasion of three-dimensional melanoma spheroids into collagen matrices (Figure 5 and Supplementary Figure S5). This dose did not kill the melanoma cells, as evident from their recurrent invasion after drug withdrawal (Figure 5 and Supplementary Figure S6). Notably, *NUMB* KD reduced the anti-invasive effects of the GSK-3 inhibitor IX (Figure 5). These data suggest that GSK-3 inhibition suppresses melanoma invasion in a NUMB-dependent manner.

The regulation of NUMB in invasion activity through the cell cycle

To investigate the potential mechanism by which NUMB regulates invasion in melanoma, we performed quantitative real time-PCR to evaluate the expression of *CCNE* and *MITF* in WM1799 and WM3451. *CCNE* and *MITF* regulate the cell cycle, cell survival, and invasion and have also been reported to be regulated by the *NUMB–NOTCH* axis (Li et al., 2014; Schmit et al., 2012; Wu et al., 2014; Zender et al., 2013).

with that in the control cell lines. Bar = 200 μm. 3D, three-dimensional; pix, pixel; shLuc, short hairpin RNA targeting firefly luciferase; shNUMB, short hairpin RNA targeting *NUMB*; shRNA, short hairpin RNA.

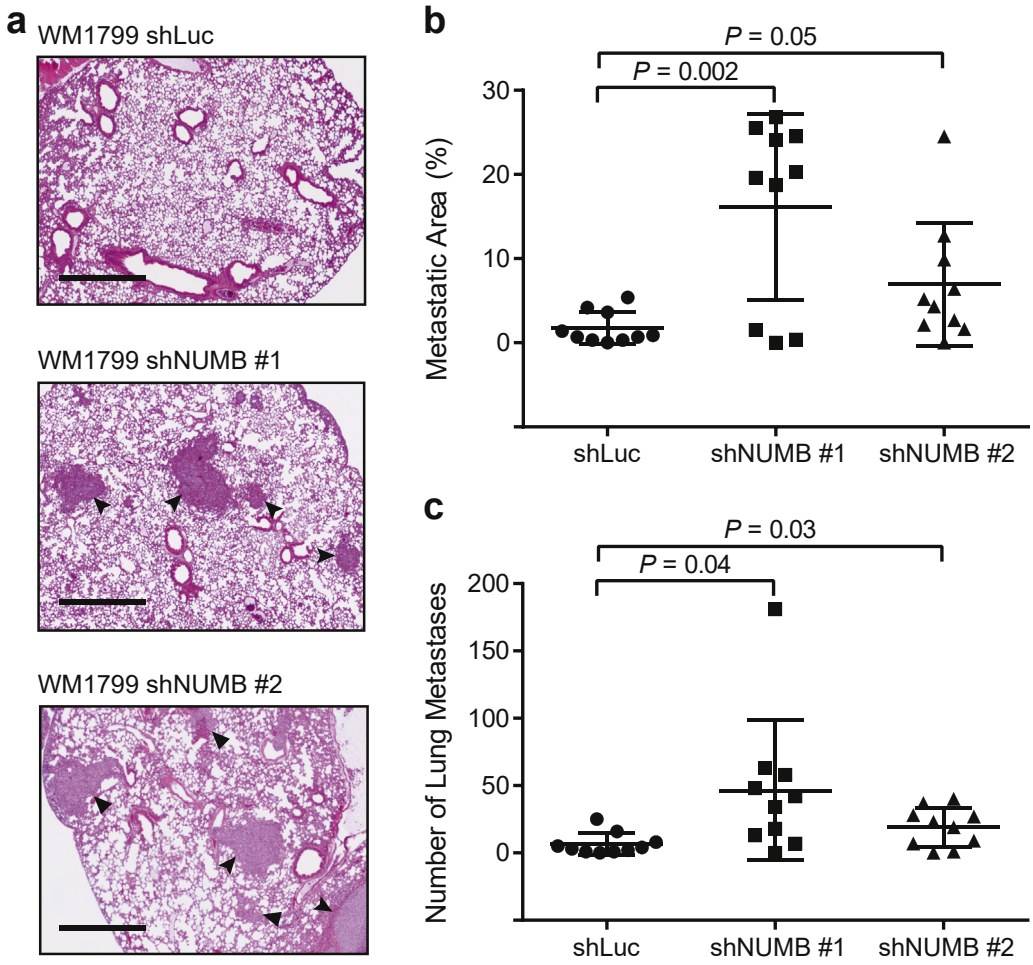

Figure 3. Knockdown of *NUMB* promotes melanoma metastasis in vivo. (**a**) H&E staining of lung tissue sections showing metastatic lesions in in vivo metastasis assays. Mice were injected intravenously with WM1799 melanoma cells transduced with a control shRNA or with shRNAs targeting *NUMB*. Arrowheads indicate metastasis. Bar = 1 mm. (**b**) Quantification of the percentage of metastatic area per lung tissue section (n = 10). (**c**) Quantification of the number of lung metastases per mouse lung section (n = 10). shLuc, short hairpin RNA targeting firefly luciferase; shRNA, short hairpin RNA.

NUMB KD increased the expression of *CCNE* in WM1799 and WM3451, whereas *NUMB* KD did not affect the expression of *MITF* (Figure 6a and b). The regulation of NUMB in invasion may thus be dependent on the cell cycle (Figure 6), which is consistent with previous reports showing the cell cycle–dependent regulation of NUMB in invasion activity (Li et al., 2014; Schmit et al., 2012; Wu et al., 2014; Zender et al., 2013).

DISCUSSION

In this study, we investigated the role of NUMB in the aggressive behavior of melanoma and its associated molecular mechanisms. NUMB is highly expressed in normal melanocytes and primary melanoma cells, whereas its expression is decreased in metastatic, aggressive melanoma cells. The analysis of The Cancer Genome Atlas dataset revealed that low NUMB expression was associated with poor overall survival. Through loss-of-function experiments, we show that NUMB downregulation leads to increased cell invasion and high metastatic capability. Furthermore, NUMB downregulation increased the expression of the *NOTCH* target gene *CCNE*, which is implicated in melanoma invasion and metastasis (Bales et al., 2005).

In terms of treatment for melanoma, immune checkpoint inhibitors play a crucial role by dramatically improving the treatment outcome of malignancies. However, the response rates of immune checkpoint inhibitors against melanoma are insufficient, and new therapeutic strategies now need to be identified for patients with melanoma (Fukumoto et al., 2021). Melanoma cells and neural crest–like skin precursors share many biological properties, such as migratory ability, self-renewal capability, and the expression of neural crest markers. Recent studies suggest that targeting neural crest–specific pathways provides an untapped reservoir of novel options (Shakhova et al., 2012; White et al., 2011). NUMB is an adaptor protein that interferes with the NOTCH pathway and has been characterized as a fate determinant during the development of an organism (Cohen and Hyman, 1994). Our previous study identified NUMB as a critical molecule in melanocyte differentiation from neural crest–like skin precursors (Fukunaga-Kalabis et al., 2015). Meanwhile, the self-renewal of neural crest–like skin precursors was shown to be controlled by NOTCH activation. Bringing these molecular players all together, the canonical Wnt stimulation was shown to upregulate NUMB, thereby inhibiting the NOTCH pathway. The

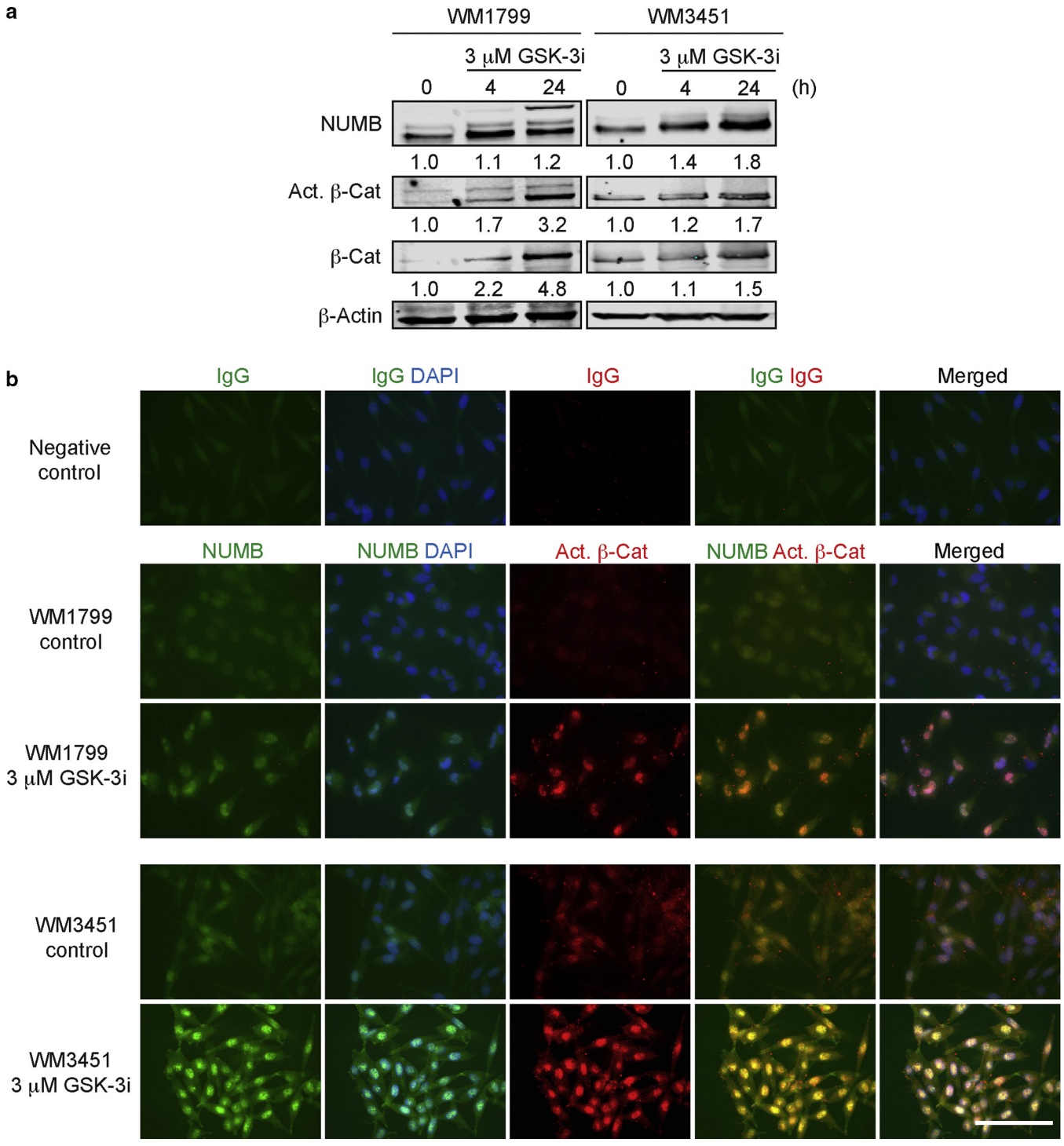

Figure 4. Inhibition of GSK-3 upregulates NUMB in metastatic melanoma cell lines. (**a**) Immunoblot analysis showing the expression of NUMB, active β-Cat, and total β-Cat in WM1799 and WM3451 melanoma cell lines treated with GSK-3i IX. The 0 h–treated samples refer to the cells incubated for 24 h in the media without GSK-3i IX. Blotting for β-actin serves as a loading control. The relative intensities of the immunoblot bands were quantified. (**b**) Immunofluorescent staining showing the expression of NUMB and active β-catenin after treatment with GSK-3i IX in WM1799 and WM3451 melanoma cell lines. Bar = 100 μm. β-Cat, β-catenin; Act., active; GSK-3, glycogen synthase kinase-3; GSK-3i, glycogen synthase kinase-3 inhibitor; h, hour.

suppression of NOTCH signaling reportedly triggers the exit from self-renewal circuitry and promotes melanocyte differentiation. Such NUMB induction and consequent repression of NOTCH signaling by canonical Wnt ligands have also been reported in chick somitic myogenesis (Holowacz et al., 2006).

In melanoma, the NOTCH pathway plays pivotal roles in the development, growth, survival, and progression of tumor cells (Bedogni, 2014). Among several NOTCH inhibitory agents, γ-secretase inhibitors have shown antitumor effects in preclinical in vivo models. However, clinical trials using these agents have been hampered by substantial toxicities at

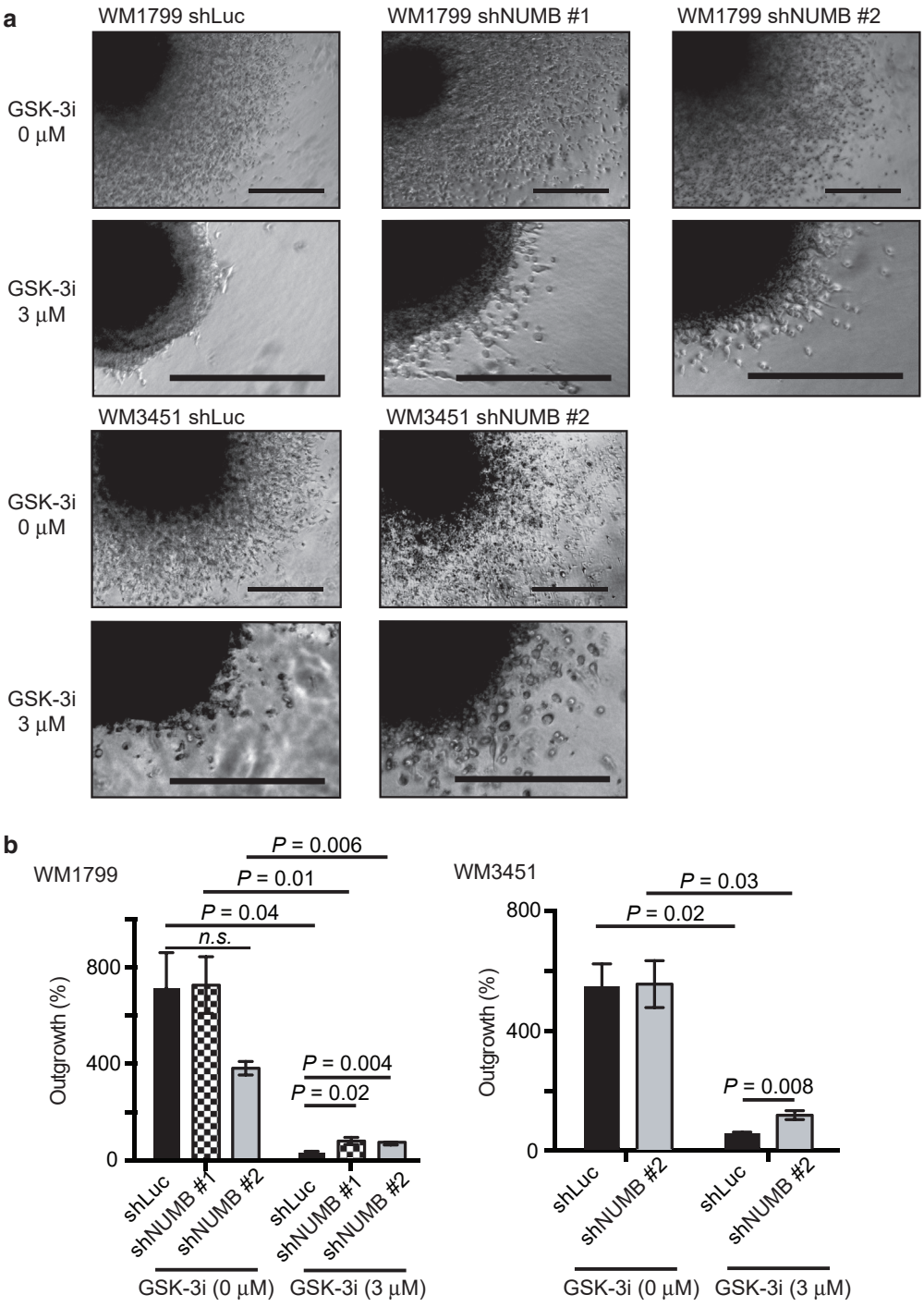

Figure 5. Knockdown of *NUMB* rescues cell invasion in melanoma cells treated with GSK-3i. (**a, b**) Control WM1799 cells (WM1799 shLuc) or WM1799 cells transduced with shNUMB (WM1799 shNUMB #1 and #2) were grown as spheroids, embedded in 3D collagen gel, and allowed to invade with or without GSK-3i IX at 3 μM for 11 days. Control WM3451 cells (WM3451 shLuc) or WM3451 cells transduced with shNUMB (WM3451 shNUMB #2) were grown as spheroids, embedded in 3D collagen gel, and allowed to invade with or without the presence of GSK-3i IX at 3 μM for 8 days. Bars = 200 μm. 3D, three-dimensional; GSK-3i, glycogen synthase kinase-3 inhibitor; n.s., not significant; shLuc, short hairpin RNA targeting firefly luciferase; shNUMB, short hairpin RNA targeting *NUMB*.

higher doses required for inhibiting the NOTCH pathway in tumors, when used as single agents (Takebe et al., 2014). Because many mechanisms contribute to NOTCH activation, the effective targeting of the pathway requires a more detailed understanding of pathway regulation and in a context-specific manner (Rizzo et al., 2008). In addition, the associated molecular players and pathways have not yet been fully investigated in melanoma and may provide encouraging results in the clinics.

Importantly, our study shows that NUMB expression can be increased by directly inhibiting a serine/threonine protein kinase, GSK-3, using a small-molecule compound. Aberrant GSK-3 signaling has been reported in numerous cancer types, and GSK-3 is highly expressed in melanoma tissues (John et al., 2012; Madhunapantula et al., 2013). In preclinical melanoma models, the inhibition of GSK-3 decreased cell proliferation, reduced migration and metastasis, and enhanced apoptosis (Atkinson et al., 2015; John et al., 2012; Kubic et al., 2012; Panka et al., 2008; Smalley et al., 2007; Zimmerman et al., 2013). Our data now show that NUMB is a pivotal mediator in the suppression of invasion by GSK-3 inhibitors. Depletion of NUMB can lead to the increased

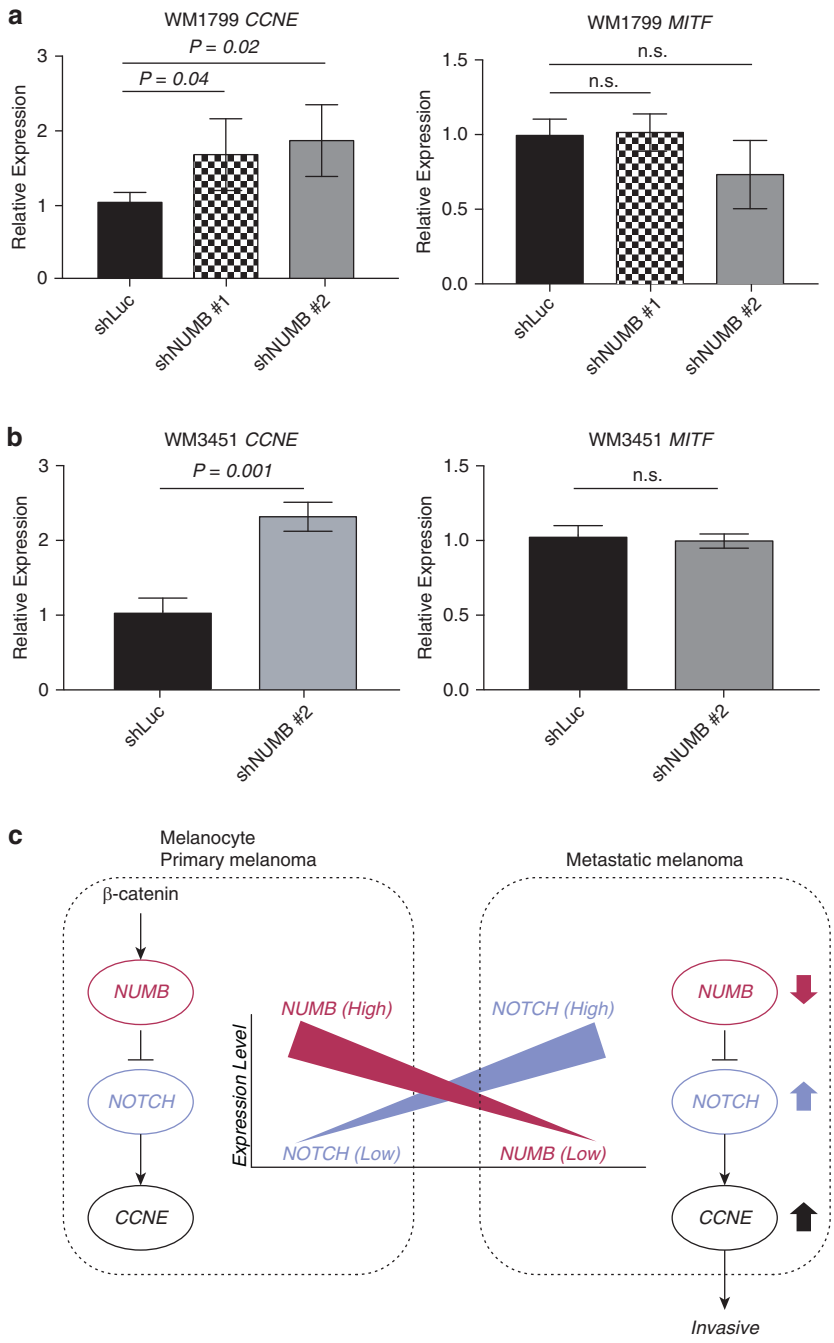

Figure 6. The effects of *NUMB* knockdown on *CCNE* and *MITF* expression. (**a, b**) Quantitative real time-PCR showing the expression of *CCNE* and *MITF* in the metastatic melanoma cell lines (**a**) WM1799 and (**b**) WM3451 transduced with shNUMB #1 and #2 compared with that in shLucs. mRNA levels of *CCNE* and *MITF* were normalized to that of *GAPDH*. (**c**) The potential mechanism of NUMB to regulate invasion activity in melanocyte and melanoma through the *NUMB–NOTCH–CCNE* axis. n.s., not significant; shLuc, short hairpin RNA targeting firefly luciferase; shNUMB, short hairpin RNA targeting *NUMB*.

expression of NOTCH target genes, which are implicated as therapeutic targets in the invasion of cancer cells (Binda et al., 2017; Tsuru et al., 2015; Weeraratna et al., 2002).

Emerging evidence shows that NUMB participates in invasion and proliferation, but the details remain controversial. Some studies reported that NUMB inhibits invasion and proliferation (Li et al., 2019; Liang et al., 2019); other conflicting studies reported that NUMB promotes cell growth (Schmit et al., 2012; Wu et al., 2014). The conclusions may depend on the variety of NUMB isoforms present or the types of cell lines or specific stages of cell development, and further studies are needed to elucidate the complexity of NUMB regulation in different biological settings (Choi et al., 2021; Colaluca et al., 2018; Liang et al., 2019; Schmit et al., 2012; Wu et al., 2014). NUMB negatively regulates the *NOTCH* target gene *CCNE* (Li et al., 2014; Zender et al., 2013). Importantly, *CCNE* has been reported to be critical for progression of cancers, including melanoma (Bales et al., 2005). Together with our current findings, we suggest that NUMB suppresses invasion and metastasis in melanoma potentially through the *NUMB–NOTCH–CCNE* axis that regulates the cell cycle (Figure 6c). Furthermore, the target-specific inhibitors that can upregulate NUMB such as GSK-3 may exert useful therapeutic effects in aggressive melanomas.

One limitation is that the mechanism by which GSK-3 inhibition increases NUMB levels remains to be elucidated.

Previous studies suggested that GSK-3 targets multiple substrates in addition to negatively regulating β-catenin signaling (Sutherland, 2011). For example, the MDM2 oncoprotein is one of the targets of GSK-3; therefore, GSK-3 inhibition leads to the hypophosphorylation of MDM2 and p53 stabilization (Kulikov et al., 2005). Interestingly, MDM2 mediates the ubiquitination and degradation of the NUMB protein (Yogosawa et al., 2003). Because MDM2 overexpression is an independent predictor of survival in patients with melanoma (Polsky et al., 2002), it is possible that GSK-3 regulates NUMB expression in an MDM2-dependent manner.

MATERIALS AND METHODS

Cell culture and reagents

Melanoma cell lines were established from melanoma specimens that were obtained in accordance with consent procedures approved by the Internal Review Boards of the Perelman School of Medicine at the University of Pennsylvania (Philadelphia, PA) and The Wistar Institute (Philadelphia, PA). Human foreskin specimens were obtained from the Cooperative Human Tissue Network (http://www.chtn.nci.nih.gov). Written informed consent was obtained when collecting tissues from patients according to the policies and procedures of the Cooperative Human Tissue Network, complying with federal human subjects regulations. The Wistar institutional review board approved foreskin sample collection from the Cooperative Human Tissue Network.

Human melanoma cells (WM1799, 1205Lu, WM3918, WM3451, WM35, WM1366, and WM3211) were isolated as previously described and cultured in 2% Mel (Satyamoorthy et al., 1997) or in melanocyte differentiation media (Li et al., 2010) supplemented with 20 ng/ml of recombinant Wnt3a or Wnt7a (R&D Systems, Minneapolis, MN). Human primary melanocytes were isolated from neonatal foreskins as previously described (Hsu et al., 2005) and cultured in 254CF media (Life Technologies, Carlsbad, CA). Lentiviral particles were produced in human embryonic kidney 293T cells, which were cultured in DMEM (Life Technologies) supplemented with 10% fetal bovine serum. The GSK-3 inhibitor IX was purchased from Calbiochem (EMD Millipore, Billerica, MA).

Lentiviral constructs

Lentiviral constructs encoding small hairpin RNA sequences targeting NUMB were purchased from GE Dharmacon (Lafayette, CO) (oligo identifications: TRCN 0000007227 and TRCN0000007226, referred to as shNUMB_1 and shNUMB_2, respectively). A lentiviral construct encoding small hairpin RNA sequences targeting luciferase (SHC007, Sigma-Aldrich, St. Louis, MO) served as vector control.

Western blot analysis

Western blotting was performed as previously described elsewhere (Fukunaga-Kalabis et al., 2015). Whole-cell lysates were generated by washing the cells with PBS and lysed with radioimmunoprecipitation assay buffer. Nuclear and cytoplasmic fraction proteins were isolated using the NE-PER Nuclear Protein Extraction Kit (Thermo Fisher Scientific, Fremont, CA) following the manufacturer's instructions. Proteins were separated on 10% polyacrylamide gels and blotted onto polyvinylidene difluoride membranes using a Trans-Blot Turbo Transfer System (Bio-Rad Laboratories, Berkeley, CA). Primary antibodies for NUMB (catalog number ab14140, dilution 1:1,000; Abcam, Cambridge, MA), active-β-catenin, 8E7 (catalog number 05-665, dilution 1:1,000; EMD Millipore), β-catenin (catalog number 610153, dilution 1:1,000; BD Biosciences, Franklin Lakes, NJ), NOTCH1 (D6F11) XP (catalog number 4380, dilution 1:1,000; Cell Signaling Technology, Danvers, MA), β-actin (catalog number A5441, dilution 1:5,000; Sigma-Aldrich), HSP90 (C45G5) (catalog number 4877, dilution 1:1,000; Cell Signaling Technology), and lamin A/C (catalog number 2032, dilution 1:1,000; Cell Signaling Technology) were used for membrane hybridization. Signals from IRDye (LI-COR Biosciences, Lincoln, NE) secondary antibodies were detected using the LI-COR Odyssey Infrared Imaging System (LI-COR Biosciences).

Quantification of morphological changes

Using ImagePro Plus software (Media Cybernetics, Rockville, MA), lines were drawn along the longest axis of the cells to measure the cell length. At least 20 cells were analyzed per condition. The length was expressed in pixels.

Three-dimensional spheroid assays

Melanoma spheroids were prepared as previously described (Smalley et al., 2006). Briefly, 5,000 melanoma cells were plated per well into a 96-well plate coated with 1.5% agar (catalog number DF0142-15-2; BD Difco, Hampton, NH). After the cells formed three-dimensional spheroid structures, the spheroids were embedded in bovine collagen I (Organogenesis, Canton, MA) containing 9% 10× EMEM (catalog number 12-684F; Lonza, Basel, Switzerland), 0.8% 200 mM L-glutamine (catalog number 25030024; Thermo Fisher Scientific, Waltham, MA), 10% fetal bovine serum, and 1.7% sodium bicarbonate (7.5% stock, catalog number 17-613E; Thermo Fisher Scientific). Spheroids were imaged with a Nikon TE2000 inverted microscope, using a Q-Imaging Retiga EX digital camera and ImagePro Plus software. The growth of the spheroids was quantified using ImagePro Plus software (Media Cybernetics). One representative spheroid from each well was selected. Then, the spheroid core and outgrowth areas were measured in square micrometer, and the percentage of outgrowth (the value reported in the analysis) was calculated as the ratio of the spheroid outgrowth to the spheroid core.

Quantitative real time-PCR

mRNAs from cells were collected using QIAshredder (Qiagen, Hilden, Germany) and the RNeasy kit (Qiagen) following the manufacturer's instructions. cDNA was synthesized from mRNA using the Maxima First Strand cDNA Synthesis Kit (Thermo Fisher Scientific) according to the manufacturer's instructions. Fast SYBR Green Master Mix (Applied Biosystems, Wilmington, DE) was used to perform quantitative real-time PCR on a 7500 Fast Real-Time PCR System (Applied Biosystems). The obtained values were normalized to *GAPDH* expression. The following primers for target genes were purchased from Integrated DNA Technologies (Coralville, IA): forward 5′-CCGGCATGCTCCAATTG-3′ and reverse 5′-TCTGGCTAAGAGCAGGAAAACC-3′ for *NUMB*, forward 5′- CCCATCATGC CGAGGGAG-3′ and reverse 5′- TATTGTCCCAAGGCTGGCTC-3′ for *CCNE*, forward 5′- AAACCCCACCAAGTACCACA-3′ and reverse 5′-ACATGGCAAGCTCAGGAC-3′ for *MITF*, and forward 5′-CTCCTTATCGTGTGGGCAGT-3′ and reverse 5′-CTTCATCCTCTCGGATCTGC-3′ for *AXIN2*.

Cell proliferation assays

First, 1×10^3 cells per well were seeded in 96 well-plates. On days 1, 4, and 6, CellTiter 96 AQueous MTS reagent (Promega, Madison, WI) was added to each well according to the manufacturer's

instructions. After 4 hours of incubation at 37 °C, the absorbance was measured at 490 nm.

Immunofluorescence staining

Cells were seeded at 4−6 × 10^4 cells/well in fibronectin-coated four-well glass chamber slides in 2% Mel melanoma growth media. The cells were fixed with 2% paraformaldehyde in PBS for 10 minutes at room temperature. Incubation with 0.2% Triton X-100 for 5 minutes at room temperature was used to permeabilize the cells. After blocking with 2% BSA for 30 minutes at room temperature, cells were incubated with primary antibodies specific for NUMB (catalog number ab14140, dilution 1:250; Abcam) and active β-catenin, 8E7 (catalog number 05-665, dilution 1:250; EMD Millipore). Alexa Fluor 488 goat anti-rabbit IgG H&L (catalog number A11034, 1:500; Life Technologies) and Alexa Fluor 555 goat anti-mouse IgG (H &L) (catalog number A21424, 1:500; Life Technologies) were used as secondary antibodies. Microscopy and photocapture were performed with a Nikon Eclipse 80i upright fluorescence microscope, using a Q Imaging EXI Aqua digital camera and ImagePro Plus 7.0 software.

Murine experimental metastasis assay

Animal experiments were performed with the approval of the Institutional Animal Care and Use Committee of The Wistar Institute in a facility accredited by the Association for the Assessment and Accreditation of Laboratory Animal Care. Subconfluent cultures of WM1799 short hairpin RNA targeting firefly luciferase, WM1799 shNUMB #1, and WM1799 shNUMB #2 melanoma cells were harvested, washed, and resuspended in sterile PBS. Approximately 100,000 cells per mouse were injected into the tail veins of non-obese diabetic/severe combined immunodeficient IL-2 receptor-γ chain null mice. Mice were killed on day 63, and the lungs were removed, washed in PBS, and fixed in 10% formalin. Tissues were embedded in paraffin, sectioned, and stained with H&E. Lung metastases were confirmed by histological analysis.

Statistics

All experiments were performed with replicate samples and were repeated two or three times for validation unless otherwise stated. The data are represented as mean ± SD. To see whether any changes between control and shNUMB#1 and/or between control and shNUMB#2 were significant, we performed two-sample *t*-tests. All statistical tests were performed with a $P \leq 0.05$ to reject the null hypothesis.

Data availability statement

All data are available in the main text or in the Supplementary Materials and Methods.

ORCIDs

Denitsa M. Hristova: http://orcid.org/0000-0001-8880-0595
Takeshi Fukumoto: http://orcid.org/0000-0003-0364-711X
Chihiro Takemori: http://orcid.org/0000-0002-9104-7474
Le Gao: http://orcid.org/0000-0003-2625-8774
Xia Hua: http://orcid.org/0000-0003-0923-6493
Joshua X. Wang: http://orcid.org/0000-0002-9949-798X
Ling Li: http://orcid.org/0000-0003-1847-4522
Marilda Beqiri: http://orcid.org/0000-0002-9738-0243
Andrea Watters: http://orcid.org/0000-0003-3810-0675
Adina Vultur: http://orcid.org/0000-0003-0068-9496
Yusra Gimie: http://orcid.org/0000-0002-3907-2904
Vito Rebecca: http://orcid.org/0000-0001-8124-0900
Anastasia Samarkina: http://orcid.org/0000-0003-1553-4366
Haruki Jimbo: http://orcid.org/0000-0003-4411-7561
Chikako Nishigori: http://orcid.org/0000-0002-6784-2849
Jie Zhang: http://orcid.org/0000-0003-0242-8812
Chaoran Cheng: http://orcid.org/0000-0001-8128-5260
Zhi Wei: http://orcid.org/0000-0001-6059-4267
Rajasekharan Somasundaram: http://orcid.org/0000-0002-8444-8472
Mizuho Fukunaga-Kalabis: http://orcid.org/0000-0001-5699-6941
Meenhard Herlyn: http://orcid.org/0000-0003-0839-0739

CONFLICT OF INTEREST

The authors state no conflict of interest.

ACKNOWLEDGMENTS

The authors thank J. Hayden and F. Keeney (Wistar Imaging Facility) and D. Gourevitch (Wistar Histology Facility) and K. Tagawa (Kobe University, Kobe, Japan) for providing technical support. The research reported in this publication was supported by the National Cancer Institute of the National Institutes of Health under award numbers R21 CA191742 (MFK), RO1 CA238237 and CA259295 (MH), U54 CA224070 (MH), and PO1 CA114046 (MH); Dr Miriam and Sheldon G Adelson Medical Research Foundation; Japan Society for the Promotion of Science KAKENHI (grant number JP20309138, TF); the Okinaka Memorial Institute for Medical Research (TF); a research grant of the Japanese Association of Geriatric Dermatology (TF); The Nakatomi Foundation (TF); and Hoansha Foundation (TF). The support for Shared Resources utilized in this study was provided by the Cancer Center Support Grant CA010815 to The Wistar Institute (Philadelphia, PA). Support for core facilities utilized in this study was provided by the Cancer Center Support Grant CA010815 to the Wistar Institute.

AUTHOR CONTRIBUTIONS

Conceptualization: TF, MFK, MH; Formal Analysis: DMH, TF, CT, LG, XH, JXW, LL, MB, AW, AV, YG, VR, AS, HJ, CN, JZ, CC, ZW, RS, MFK, MH; Funding Acquisition: TF, MFK, MH; Investigation: DMH, TF, CT, LG, XH, JXW, LL, MB, AW, AV, YG, VR, AS, HJ, CN, JZ, CC, ZW, RS, MFK, MH; Methodology: DMH, TF, CT, LG, XH, JXW, LL, MB, AW, AV, YG, VR, AS, HJ, CN, JZ, CC, ZW, RS, MFK, MH; Resources: TF, MFK, MH; Supervision: TF, MFK, MH; Validation: DMH, TF, CT, LG, XH, JXW, LL, MB, AW, AV, YG, VR, AS, HJ, CN, JZ, CC, ZW, RS, MFK, MH; Visualization: DMH, TF, MFK, MH; Writing - Original Draft Preparation: DMH, TF, MFK, MH

Disclaimer

The content of this study is solely the responsibility of the authors and does not necessarily represent the official views of the National Institutes of Health.

SUPPLEMENTARY MATERIAL

Supplementary material is linked to the online version of the paper at www.jidonline.org, and at https://doi.org/10.1016/j.jid.2021.11.027.

REFERENCES

Atkinson JM, Rank KB, Zeng Y, Capen A, Yadav V, Manro JR, et al. Activating the Wnt/β-catenin pathway for the treatment of melanoma–application of LY2090314, a novel selective inhibitor of glycogen synthase kinase-3. PLoS One 2015;10:e0125028.

Aydin IT, Melamed RD, Adams SJ, Castillo-Martin M, Demir A, Bryk D, et al. FBXW7 mutations in melanoma and a new therapeutic paradigm. J Natl Cancer Inst 2014;106:dju107.

Bales E, Mills L, Milam N, McGahren-Murray M, Bandyopadhyay D, Chen D, et al. The low molecular weight cyclin E isoforms augment angiogenesis and metastasis of human melanoma cells in vivo. Cancer Res 2005;65:692−7.

Balint K, Xiao M, Pinnix CC, Soma A, Veres I, Juhasz I, et al. Activation of Notch1 signaling is required for beta-catenin-mediated human primary melanoma progression. J Clin Invest 2005;115:3166−76.

Bedogni B. Notch signaling in melanoma: interacting pathways and stromal influences that enhance Notch targeting. Pigment Cell Melanoma Res 2014;27:162−8.

Binda E, Visioli A, Giani F, Trivieri N, Palumbo O, Restelli S, et al. Wnt5a drives an invasive phenotype in human glioblastoma stem-like cells [published correction appears in Cancer Res 2017;77:3962]. Cancer Res 2017;77:996−1007.

Cancer Genome Atlas Network. Genomic classification of cutaneous melanoma. Cell 2015;161:1681−96.

Cheng G, He J, Zhang L, Ge S, Zhang H, Fan X. HIC1 modulates uveal melanoma progression by activating lncRNA-numb. Tumour Biol 2016;37:12779−89.

Choi HY, Seok J, Kang GH, Lim KM, Cho SG. The role of NUMB/NUMB isoforms in cancer stem cells. BMB Rep 2021;54:335–43.

Cohen S, Hyman AA. Cell fate determination. When is a determinant a determinant? Curr Biol 1994;4:420–2.

Colaluca IN, Basile A, Freiburger L, D'Uva V, Disalvatore D, Vecchi M, et al. A Numb-Mdm2 fuzzy complex reveals an isoform-specific involvement of Numb in breast cancer. J Cell Biol 2018;217:745–62.

Colaluca IN, Tosoni D, Nuciforo P, Senic-Matuglia F, Galimberti V, Viale G, et al. NUMB controls p53 tumour suppressor activity. Nature 2008;451:76–80.

Di Marcotullio L, Ferretti E, Greco A, De Smaele E, Po A, Sico MA, et al. Numb is a suppressor of Hedgehog signalling and targets Gli1 for itch-dependent ubiquitination. Nat Cell Biol 2006;8:1415–23.

Forloni M, Dogra SK, Dong Y, Conte D Jr, Ou J, Zhu LJ, et al. miR-146a promotes the initiation and progression of melanoma by activating Notch signaling. Elife 2014;3:e01460.

Fukumoto T, Lin J, Fatkhutdinov N, Liu P, Somasundaram R, Herlyn M, et al. ARID2 deficiency correlates with the response to immune checkpoint blockade in melanoma. J Invest Dermatol 2021;141:1564–72.e4.

Fukunaga-Kalabis M, Hristova DM, Wang JX, Li L, Heppt MV, Wei Z, et al. UV-induced Wnt7a in the human skin microenvironment specifies the fate of neural crest-like cells via suppression of notch. J Invest Dermatol 2015;135:1521–32.

Holowacz T, Zeng L, Lassar AB. Asymmetric localization of numb in the chick somite and the influence of myogenic signals. Dev Dyn 2006;235:633–45.

Hsu MY, Li L, Herlyn M. Cultivation of normal human epidermal melanocytes in the absence of phorbol esters. Methods Mol Med 2005;107:13–28.

John JK, Paraiso KH, Rebecca VW, Cantini LP, Abel EV, Pagano N, et al. GSK3β inhibition blocks melanoma cell/host interactions by down-regulating N-cadherin expression and decreasing FAK phosphorylation. J Invest Dermatol 2012;132:2818–27.

Kubic JD, Mascarenhas JB, Iizuka T, Wolfgeher D, Lang D. GSK-3 promotes cell survival, growth, and PAX3 levels in human melanoma cells. Mol Cancer Res 2012;10:1065–76.

Kulikov R, Boehme KA, Blattner C. Glycogen synthase kinase 3-dependent phosphorylation of Mdm2 regulates p53 abundance. Mol Cell Biol 2005;25:7170–80.

Li JY, Huang WX, Zhou X, Chen J, Li Z. Numb inhibits epithelial-mesenchymal transition via RBP-Jκ-dependent Notch1/PTEN/FAK signaling pathway in tongue cancer. BMC Cancer 2019;19:391.

Li L, Fukunaga-Kalabis M, Yu H, Xu X, Kong J, Lee JT, et al. Human dermal stem cells differentiate into functional epidermal melanocytes. J Cell Sci 2010;123:853–60.

Li Z, Xiang Y, Xiang L, Xiao Y, Li F, Hao P. ALDH maintains the stemness of lung adenoma stem cells by suppressing the Notch/CDK2/CCNE pathway. PLoS One 2014;9:e92669.

Liang J, Han B, Zhang Y, Yue Q. Numb inhibits cell proliferation, invasion, and epithelial-mesenchymal transition through PAK1/β-catenin signaling pathway in ovarian cancer. Onco Targets Ther 2019;12:3223–33.

Liu J, Fukunaga-Kalabis M, Li L, Herlyn M. Developmental pathways activated in melanocytes and melanoma. Arch Biochem Biophys 2014;563:13–21.

Liu ZJ, Xiao M, Balint K, Smalley KS, Brafford P, Qiu R, et al. Notch1 signaling promotes primary melanoma progression by activating mitogen-activated protein kinase/phosphatidylinositol 3-kinase-Akt pathways and up-regulating N-cadherin expression. Cancer Res 2006;66:4182–90.

Madhunapantula SV, Sharma A, Gowda R, Robertson GP. Identification of glycogen synthase kinase 3α as a therapeutic target in melanoma. Pigment Cell Melanoma Res 2013;26:886–99.

Milán-Rois P, Quan A, Slack FJ, Somoza Á. The role of lncRNAs in uveal melanoma. Cancers (Basel) 2021;13:4041.

Panka DJ, Cho DC, Atkins MB, Mier JW. GSK-3beta inhibition enhances sorafenib-induced apoptosis in melanoma cell lines. J Biol Chem 2008;283:726–32.

Pece S, Confalonieri S, R Romano P, Di Fiore PP. NUMB-ing down cancer by more than just a NOTCH. Biochim Biophys Acta 2011;1815:26–43.

Polsky D, Melzer K, Hazan C, Panageas KS, Busam K, Drobnjak M, et al. HDM2 protein overexpression and prognosis in primary malignant melanoma. J Natl Cancer Inst 2002;94:1803–6.

Rizzo P, Osipo C, Foreman K, Golde T, Osborne B, Miele L. Rational targeting of Notch signaling in cancer. Oncogene 2008;27:5124–31.

Satyamoorthy K, DeJesus E, Linnenbach AJ, Kraj B, Kornreich DL, Rendle S, et al. Melanoma cell lines from different stages of progression and their biological and molecular analyses. Melanoma Res 1997;7(Suppl. 2):S35–42.

Schmit TL, Nihal M, Ndiaye M, Setaluri V, Spiegelman VS, Ahmad N. Numb regulates stability and localization of the mitotic kinase PLK1 and is required for transit through mitosis. Cancer Res 2012;72:3864–72.

Shakhova O, Zingg D, Schaefer SM, Hari L, Civenni G, Blunschi J, et al. Sox10 promotes the formation and maintenance of giant congenital naevi and melanoma. Nat Cell Biol 2012;14:882–90.

Smalley KS, Contractor R, Haass NK, Kulp AN, Atilla-Gokcumen GE, Williams DS, et al. An organometallic protein kinase inhibitor pharmacologically activates p53 and induces apoptosis in human melanoma cells. Cancer Res 2007;67:209–17.

Smalley KS, Haass NK, Brafford PA, Lioni M, Flaherty KT, Herlyn M. Multiple signaling pathways must be targeted to overcome drug resistance in cell lines derived from melanoma metastases. Mol Cancer Ther 2006;5:1136–44.

Sutherland C. What are the bona fide GSK3 substrates? Int J Alzheimers Dis 2011;2011:505607.

Takebe N, Nguyen D, Yang SX. Targeting notch signaling pathway in cancer: clinical development advances and challenges. Pharmacol Ther 2014;141:140–9.

Tsuru A, Setoguchi T, Matsunoshita Y, Nagao-Kitamoto H, Nagano S, Yokouchi M, et al. Hairy/enhancer-of-split related with YRPW motif protein 1 promotes osteosarcoma metastasis via matrix metallopeptidase 9 expression. Br J Cancer 2015;112:1232–40.

Uemura T, Shepherd S, Ackerman L, Jan LY, Jan YN. Numb, a gene required in determination of cell fate during sensory organ formation in Drosophila embryos. Cell 1989;58:349–60.

Wakamatsu Y, Maynard TM, Jones SU, Weston JA. NUMB localizes in the basal cortex of mitotic avian neuroepithelial cells and modulates neuronal differentiation by binding to NOTCH-1. Neuron 1999;23:71–81.

Weeraratna AT, Jiang Y, Hostetter G, Rosenblatt K, Duray P, Bittner M, et al. Wnt5a signaling directly affects cell motility and invasion of metastatic melanoma. Cancer Cell 2002;1:279–88.

White RM, Cech J, Ratanasirintrawoot S, Lin CY, Rahl PB, Burke CJ, et al. DHODH modulates transcriptional elongation in the neural crest and melanoma. Nature 2011;471:518–22.

Wu J, Shen SL, Chen B, Nie J, Peng BG. Numb promotes cell proliferation and correlates with poor prognosis in hepatocellular carcinoma. PLoS One 2014;9:e95849.

Yogosawa S, Miyauchi Y, Honda R, Tanaka H, Yasuda H. Mammalian Numb is a target protein of Mdm2, ubiquitin ligase. Biochem Biophys Res Commun 2003;302:869–72.

Zender S, Nickeleit I, Wuestefeld T, Sörensen I, Dauch D, Bozko P, et al. A critical role for notch signaling in the formation of cholangiocellular carcinomas [published correction appears in Cancer Cell 2016;30:353–6]. Cancer Cell 2013;23:784–95.

Zhong W, Feder JN, Jiang MM, Jan LY, Jan YN. Asymmetric localization of a mammalian numb homolog during mouse cortical neurogenesis. Neuron 1996;17:43–53.

Zimmerman ZF, Kulikauskas RM, Bomsztyk K, Moon RT, Chien AJ. Activation of Wnt/β-catenin signaling increases apoptosis in melanoma cells treated with trail. PLoS One 2013;8:e69593.

SUPPLEMENTARY MATERIALS

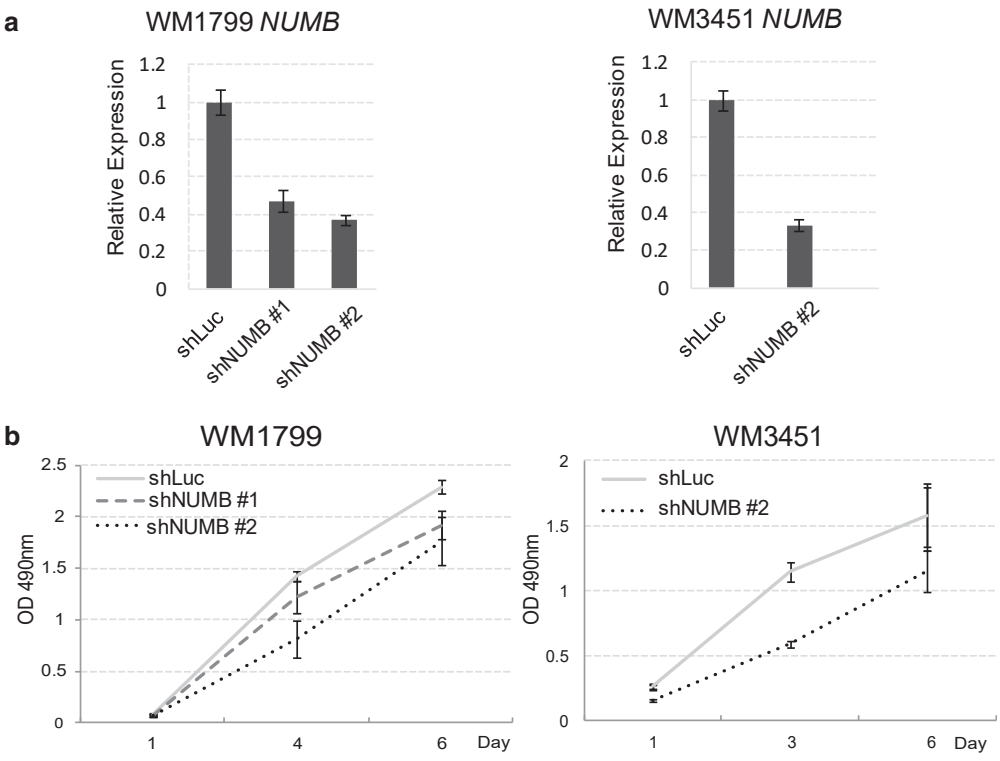

Supplementary Figure S1. Knockdown efficacy of shNUMB in metastatic melanoma cell lines. (**a**) Quantitative real time-PCR showing decreased *NUMB* mRNA levels in the metastatic melanoma cell lines WM1799 and WM3451 transduced with shNUMB #1 and #2 compared with that in shLuc. mRNA levels of *NUMB* were normalized to that of *GAPDH*. (**b**) The MTS assay was used to assess the effect of *NUMB* knockdown on cell proliferation. OD, optical density; shLuc, short hairpin RNA targeting firefly luciferase; shNUMB, short hairpin RNA targeting *NUMB*.

Supplementary Figure S2. Knockdown efficacy of shNUMB in a primary melanoma cell line. (**a**) Immunoblot analysis showing NUMB expression in a primary melanoma cell line with a control vector (shLuc) or shNUMB #1 and #2. Blotting for β-actin serves as a loading control. The relative intensities of the immunoblot bands were quantified. (**b**) Quantitative real time-PCR showing decreased *NUMB* mRNA levels in the primary melanoma cell line WM35 transduced with shNUMB #1 and #2 compared with that in shLuc. mRNA levels of *NUMB* were normalized to that of *GAPDH*. (**c**) The MTS assay was used to assess the effect of NUMB knockdown on cell proliferation. (**d**) Downregulation of *NUMB* by shRNA in primary melanoma cell lines leads to morphological changes. Bars = 200 μm. OD, optical density; shLuc, short hairpin RNA targeting firefly luciferase; shNUMB, short hairpin RNA targeting *NUMB*; shRNA, short hairpin RNA.

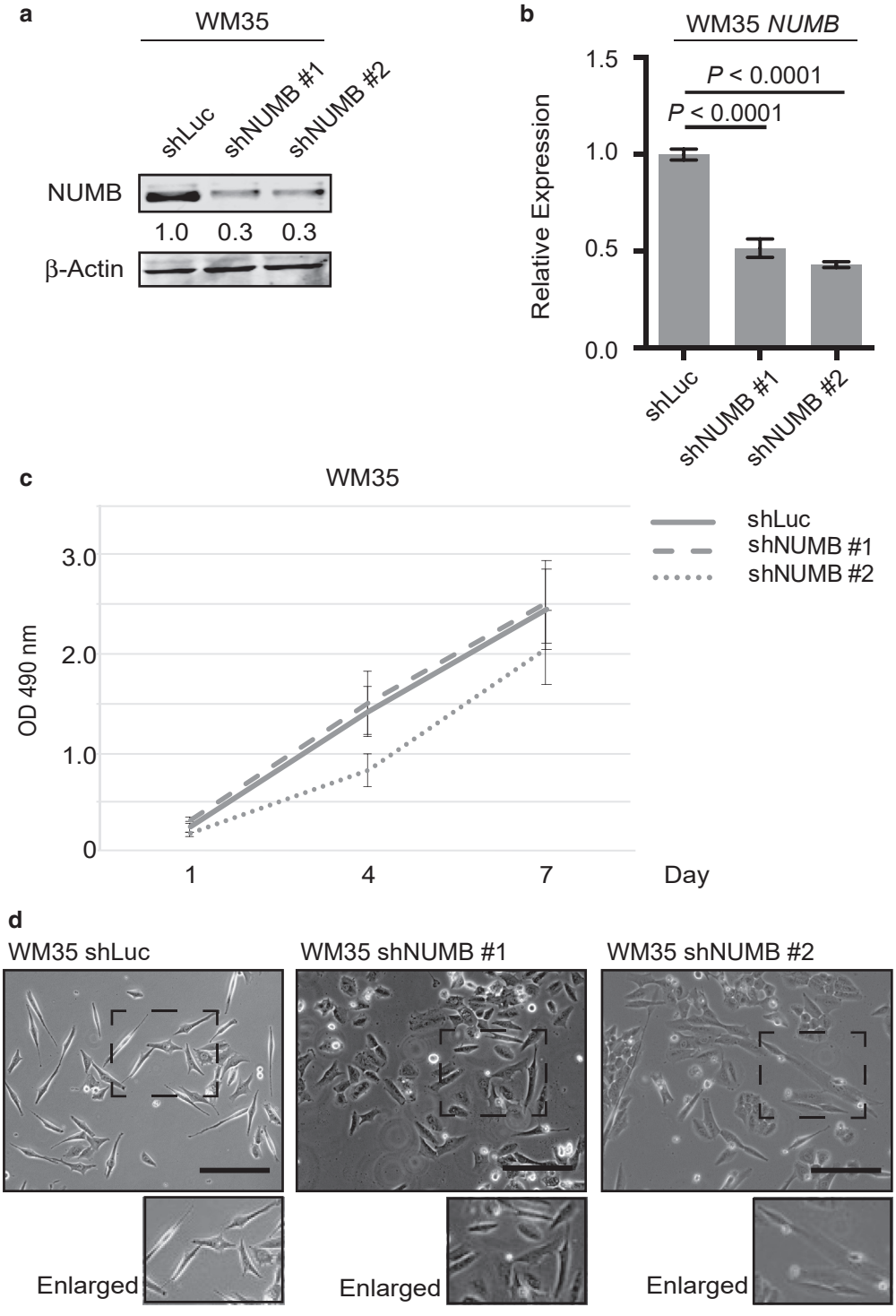

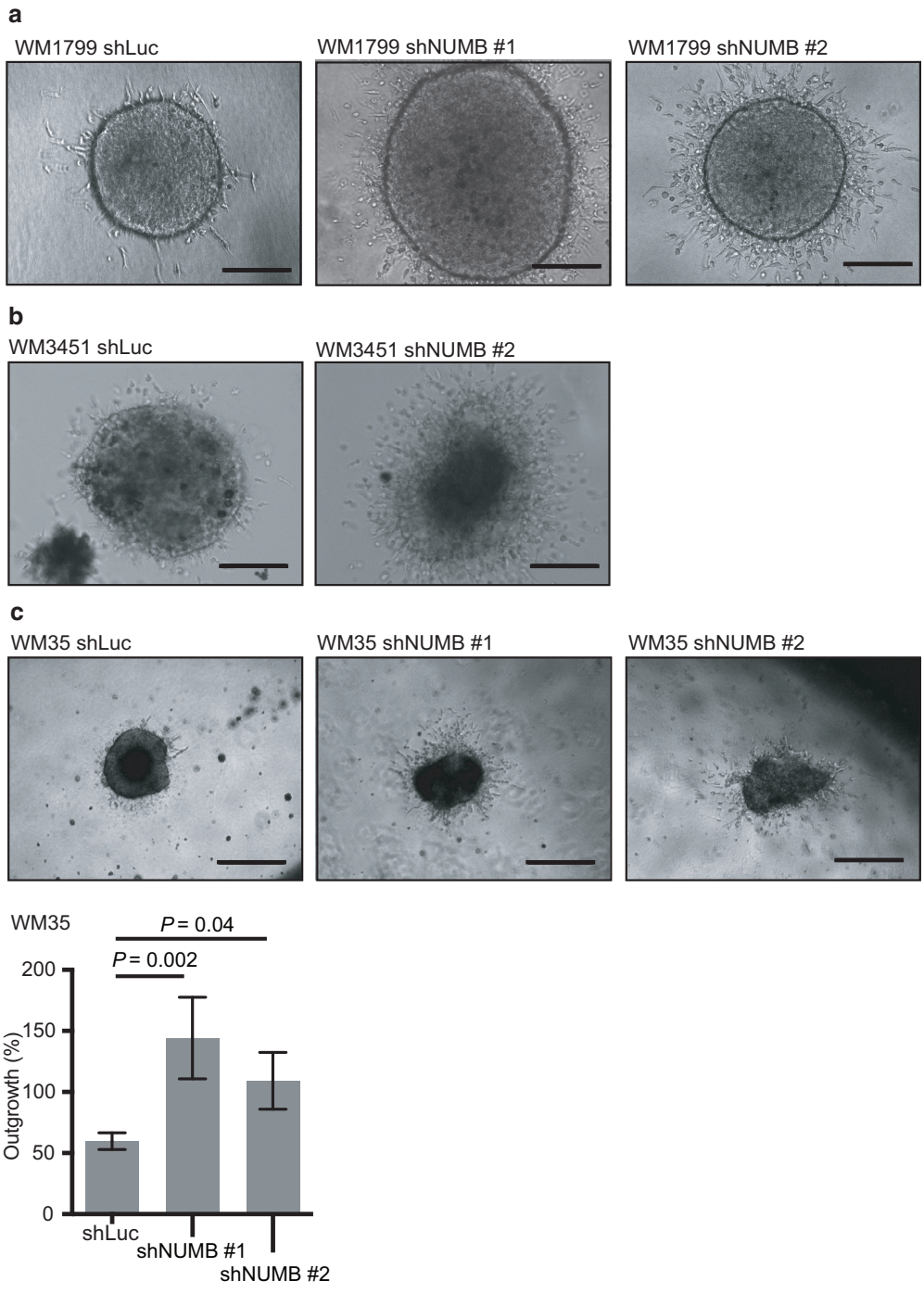

Supplementary Figure S3. Knockdown efficacy of shNUMB in a primary melanoma cell line. (**a–c**) shNUMB-transduced cells or control vector–transduced cells were grown as spheroids embedded in a 3D collagen matrix to test their invasive ability. *NUMB*-knockdown cell lines showed increased invasion in (**a**) WM1799 (on day 1) and (**b**) WM3451 (on day 2) and (**c**) WM35 (on day 4) melanoma cell lines compared with that in the control cell lines. Bars = 200 μm. 3D, three-dimensional; shLuc, short hairpin RNA targeting firefly luciferase; shNUMB, short hairpin RNA targeting *NUMB*.

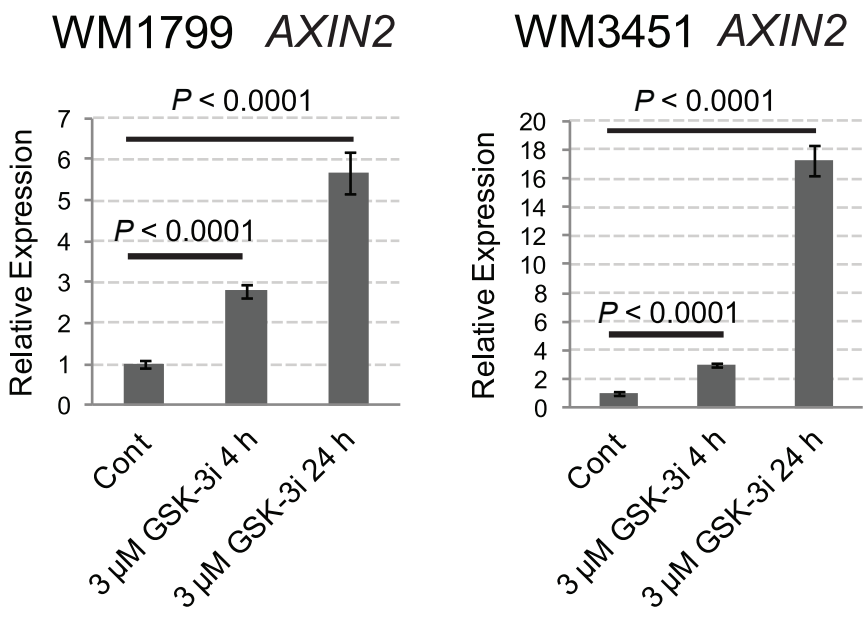

Supplementary Figure S4. *AXIN2* expression in GSK-3i–treated melanoma cells. Quantitative real time-PCR showing the time-course expression of *AXIN2*, a target gene of β-catenin, in WM1799 and WM3451 melanoma cell lines treated with GSK-3i IX at 3 μM. The mRNA levels were normalized to that of *GAPDH*. Cont, no treatment with GSK-3i; GSK-3i, glycogen synthase kinase-3 inhibitor; h, hour.

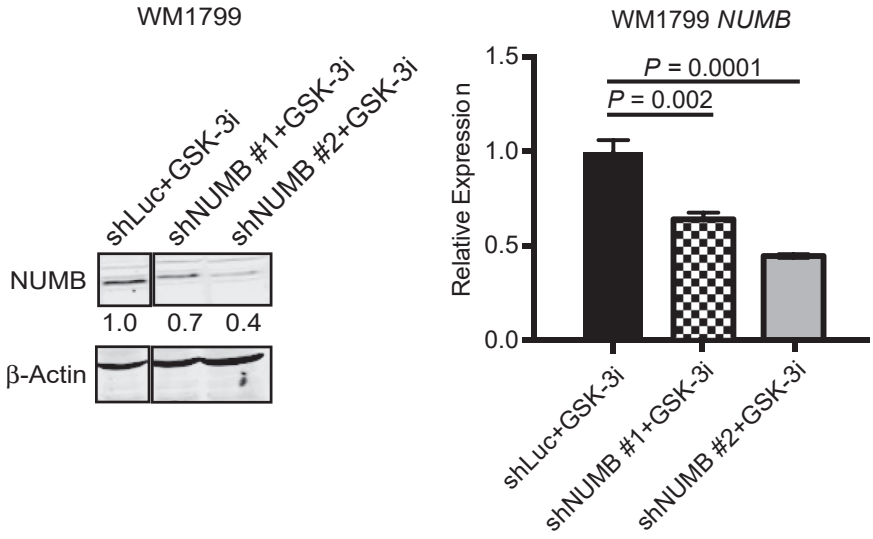

Supplementary Figure S5. The rescue efficacy of *NUMB* knockdown on GSK-3i–treated melanoma cells. (**a**) Immunoblot analysis showing NUMB expression in GSK-3 inhibitor–treated WM1799 with a control vector (shLuc) or shNUMB #1 and #2. Blotting for β-actin serves as a loading control. The relative intensities of the immunoblot bands were quantified. (**b**) Quantitative real time-PCR showing decreased *NUMB* mRNA levels in GSK-3i–treated WM1799 transduced with shNUMB #1 and #2 compared with that in shLucs. mRNA levels of *NUMB* were normalized to that of *GAPDH*. GSK-3i, glycogen synthase kinase-3 inhibitor; shLuc, short hairpin RNA targeting firefly luciferase; shNUMB, short hairpin RNA targeting *NUMB*.

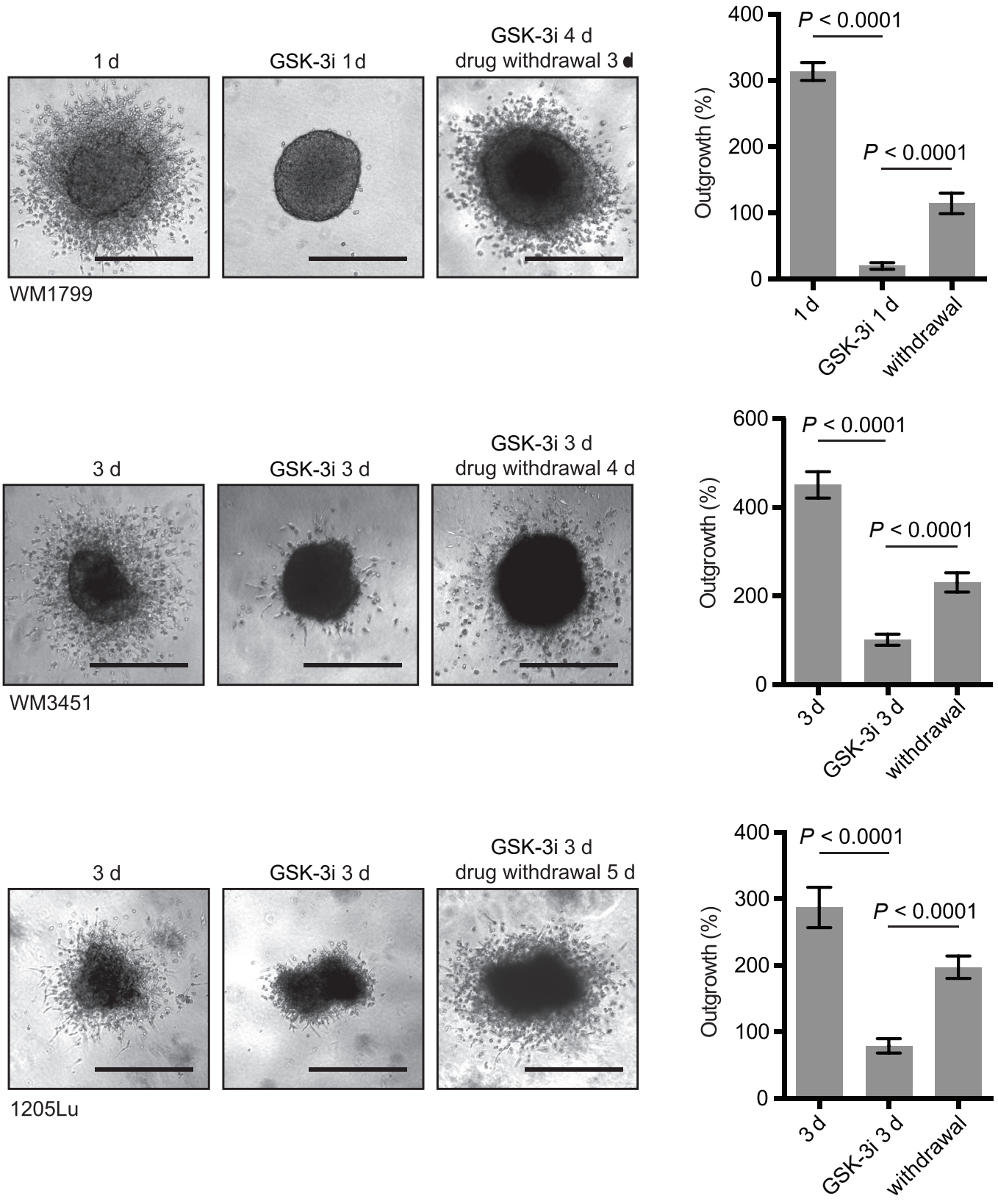

Supplementary Figure S6. Inhibition of GSK-3 reduces cell invasion in melanoma cell lines. Melanoma cell lines were grown as spheroids embedded in the collagen matrix and were allowed to invade with or without the presence of GSK-3i IX at 3 μM for 1 d or 3 d in WM1799, WM3451, and 1205Lu melanoma cell lines. Inhibition of GSK-3 resulted in delayed cell invasion at the timepoints of 1 or 3 d. After the drug was withdrawn, cells started to invade the collagen matrix. Bars = 200 μm. d, day; GSK-3i, glycogen synthase kinase-3 inhibitor.